ISBN: 978-3-95450-231-8 ISSN: 2673-5490 doi: 10.18429/JACoW-IPAC2023-MOPM065

GENERALIZED LONGITUDINAL STRONG FOCUSING IN A STORAGE RING FOR COHERENT EUV RADIATION

Z. Li, X. Deng, Z. Pan, C. Tang*,
Department of Engineering Physics, Tsinghua University, Beijing, China
A. Chao[1†], Institute for Advanced Study, Tsinghua University, Beijing, China
[1]also at Stanford University, Stanford, USA

Abstract

A laser-driven storage ring is proposed to generate steady-state, nanometer-long electron bunches. A ring of this type can produce coherent EUV radiation with greatly enhanced power and photon flux, benefiting a wide range of scientific and industrial communities, including condensed matter physics and computer chip fabrication. The underlying mechanism is called generalized longitudinal strong focusing (GLSF), which invokes precise transverse-longitudinal coupling dynamics and lowers the required laser power significantly by exploiting the ultrasmall vertical beam emittance. A practical instance indicates that kW-level coherent EUV radiation is attainable in a GLSF ring with a modulation laser power as low as 1 MW, allowing for continuous-wave operation of up-to-date optical cavities.

INTRODUCTION

Storage ring-based synchrotron radiation facilities are powerful sources of extreme ultraviolet (EUV) photons. The EUV radiation from most rings is, however, incoherent over time. Coherent EUV radiation is desired by various applications for its boosted power and photon flux. Angle-resolved photoemission spectroscopy relies on high-flux EUV photons to reveal the key electronic structures in topological materials [1]. High-power EUV sources are longed for by EUV lithography for high-volume microchip production [2].

The failure of most storage rings to produce coherent EUV radiation is due to electron bunches being too long. Scenarios for generating nanometer bunches in storage rings have then been proposed [3–6]. Distinct from conventional rings, laser modulators are used for bunching instead of RF cavities to reduce modulation wavelengths, while ring optics are tuned carefully to contain bunch lengthening from stochastic photon emission. A longitudinal strong focusing (LSF) scheme further compresses bunches by using laser modulators as longitudinal focusing elements. The required power of the modulation laser, however, exceeds the capacity of current optical cavities in continuous-wave mode.

In the attempt to generate coherent EUV radiation in a storage ring on a turn-by-turn basis, the power of the modulation laser should be controlled at the level of 1 MW that optical cavities could bear for continuous-wave mode operation. Besides, the nanometer bunch length is taken as an eigenstate of the ring. The status of electron bunches should be recovered after compression. Unlike in single-pass devices, the de-compression process is pivotal in storage rings.

* tang.xuh@tsinghua.edu.cn
† achao@slac.stanford.edu

GENERALIZED LONGITUDINAL STRONG FOCUSING (GLSF) SCHEME

In this paper, a generalized longitudinal strong focusing (GLSF) scheme is proposed to produce coherent EUV radiation turn by turn in laser-driven storage rings. In both LSF and GLSF schemes, strong manipulation is imposed to obtain nanometer bunches. The distinction lies in the way electrons are handled. Instead of manipulation in the longitudinal dimension alone, GLSF rings invoke transverse-longitudinal coupling beam dynamics. The extremely low vertical beam emittance in an uncoupled planar ring is exploited. By projecting the minimum one of the three eigen-emittances, a short bunch length can be attained with significantly reduced modulation laser power. The introduced coupling and modulation are then canceled after radiation so that an uncoupled bunch is retained and the low vertical beam emittance can be kept and used again next turn. With practical beam parameters, it can be shown that kW-level quasi-continuous-wave coherent EUV radiation is attainable turn by turn in a GLSF ring with a modulation laser power as low as 1 MW, allowing for continuous-wave operation of up-to-date optical cavities.

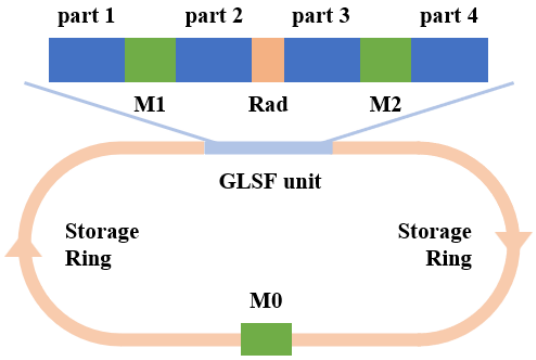

Figure 1: Sketch showing the general layout of a GLSF storage ring. The GLSF unit includes four lattice segments (parts 1-4), two modulators (M1, M2), and a radiator (Rad).

The general layout of a GLSF storage ring is sketched in Fig. 1. The GLSF unit can be decomposed into four segments of dispersive lattice separated by two modulators and one radiator. The first half of the GLSF unit handles bunch

ISBN: 978-3-95450-231-8 ISSN: 2673-5490 doi: 10.18429/JACoW-IPAC2023-MOPM065

compression at the radiator, while the de-compression (modulation cancellation and transverse-longitudinal decoupling) is accomplished by the second half. An additional laser modulator, M0, is utilized in the storage ring for pre-bunching. In principle, however, this scheme works for RF-bunched or coasting beams as well.

It should be noted that the proposed scheme has the potential to further reduce the wavelength of coherent radiation, allowing it to play a role in x-ray sciences. It could also be used in conventional rings to generate coherent THz radiation and ultrashort pulses in a novel way.

LINEAR BEAM DYNAMICS

For illustration, the 'transverse' dimension involved in coupling is assumed to be the vertical one. Thus, particle coordinates of interest are (y, y', z, δ). This section goes into detail about the linear beam dynamics of the GLSF unit, including bunch compression, modulation cancellation, vertical-longitudinal decoupling, and bunching factor.

Bunch compression

For the purpose of bunch compression by projecting the vertical emittance ϵ_y to bunch length at the radiator $\sigma_z(\mathrm{Rad})$, coupling shall be introduced, and the contribution from the longitudinal emittance ϵ_z must be eliminated.

The modulator M1 is sandwiched by two vertically dispersive lattice segments, parts 1-2. The first half of the GLSF unit can be decomposed into four key features in function: (i) (m_{36}, m_{46}) from part 1 to correlate (y, y') with δ; (ii) h generated by M1 to correlate δ with z; (iii) n_{56} from part 2 to correlate z with δ; (iv) (n_{53}, n_{54}) from part 2 to correlate z with (y, y'). Here, h is the modulation strength of M1 ($\Delta\delta = hz$). (m_{36}, m_{46}) and (n_{53}, n_{54}, n_{56}) are matrix elements of interest of the transport maps of parts 1 and 2 respectively, where subscripts $(3, 4, 5, 6)$ correspond to coordinates (y, y', z, δ). Extra terms of z_{rad} contributed from initial z_0 and δ_0 are brought out by features (ii, iii) as $\Delta z = hn_{56}z_0$ and (i, iv) as $\Delta z = (m_{36}n_{53} + m_{46}n_{54})\,\delta_0$.

Therefore, the conditions required to remove the dependence of $\sigma_z(\mathrm{Rad})$ on initial particle coordinates (z, δ) are:

$$\begin{aligned} 1 + hn_{56} &= 0, \\ m_{36}n_{53} + m_{46}n_{54} + n_{56} &= 0. \end{aligned} \tag{1}$$

When Eq. (1) is fulfilled, there is:

$$\sigma_z(\mathrm{Rad}) = \sqrt{\epsilon_y \mathcal{H}_y(\mathrm{Rad})}. \tag{2}$$

Here, $\mathcal{H}_y(\mathrm{Rad})$ is a lattice-dependent function. $\sigma_z(\mathrm{Rad})$ relies solely on vertical parameters. $\sigma_z(\mathrm{Rad}) = 3$ nm can be expected with $\epsilon_y = 1$ pm·rad and $\mathcal{H}_y(\mathrm{Rad}) = 9$ μm.

Modulation cancellation

An additional laser modulator, M2, is paired with M1, the existing one, to undo changes imposed on the beam. Their modulations are identical in waveform and amplitude yet opposite in sign. The lattice between them, parts 2-3, is made longitudinally 'transparent' to particles so that coordinates in z dimension do not change. Modulations, therefore, directly add up and cancel each other perfectly.

The transparency in the z dimension is ensured by making parts 2 and 3 as a whole both achromatic and isochronous. Note that it is not necessarily an I-map. The transportation in (y, y') phase space can be free since it does not bother the cancellation of modulation. The cancellation works for arbitrary modulation waveforms.

Vertical-longitudinal decoupling

The intention to decouple vertical and longitudinal dimensions at the end of the GLSF unit is to ensure that a low vertical emittance can be maintained and that beam status gets recovered and is ready for manipulation the following turn. Since the remaining coupling terms after modulation cancellation are dispersion-related, a final lattice segment, part 4, is left to make the entire GLSF unit an achromat.

Bunching factor

The bunching factor b_n, to whose square the power of coherent radiation is proportional, quantifies the bunching behavior of the particles. The bunching factor at the radiator in a GLSF storage ring is given by [7]:

$$b_n = e^{-\frac{1}{2}k_{\mathrm{r}}^2\sigma_z^2(\mathrm{Rad})} \left| \sum_{p=-\infty}^{\infty} J_p(n) e^{-\frac{1}{2}(n-p)^2 k_{\mathrm{m}}^2 \sigma_z^2(\mathrm{Mod})} \right|. \tag{3}$$

Here, $k_{\mathrm{r}} = \frac{2\pi}{\lambda_{\mathrm{r}}}$ is the radiation wave number, with λ_{r} the radiation wavelength. $k_{\mathrm{m}} = \frac{2\pi}{\lambda_{\mathrm{m}}}$ is the modulation wave number, with λ_{m} the modulation wavelength. $n = \frac{k_{\mathrm{r}}}{k_{\mathrm{m}}} = \frac{\lambda_{\mathrm{m}}}{\lambda_{\mathrm{r}}}$ is the harmonic number, and J_p is the p-th order Bessel function of the first kind. $\sigma_z(\mathrm{Mod})$ is the bunch length measured at M1. Note that the term $e^{-\frac{1}{2}k_{\mathrm{r}}^2\sigma_z^2(\mathrm{Rad})}$ in b_n stands for the bunching factor of a Gaussian-distributed beam. When considering the nonlinear nature of the *sine*-wave modulation at M1, the beam distribution is distorted at the radiator, and the bunching factor degrades. The reduction factor is the term $|\sum_{p=-\infty}^{\infty} J_p(n) e^{-\frac{1}{2}(n-p)^2 k_{\mathrm{m}}^2 \sigma_z^2(\mathrm{Mod})}|$ left in b_n.

Short bunch lengths at the radiator and modulator are desired to improve b_n. They cannot, however, be reduced to arbitrary values since their product is limited by [7]:

$$\sigma_{z\_y}(\mathrm{Mod})\sigma_z(\mathrm{Rad}) \geq \frac{\epsilon_y}{|h|}. \tag{4}$$

Here $|h|$ is the effective modulation strength from M1. $\sigma_{z\_y}(\mathrm{Mod})$ is part of $\sigma_z(\mathrm{Mod})$ contributed from ϵ_y and coupling. There is $\sigma_z(\mathrm{Mod}) = \sqrt{\sigma_{z\_y}^2(\mathrm{Mod}) + \sigma_{z\_z}^2(\mathrm{Mod})}$, where $\sigma_{z\_z}(\mathrm{Mod})$ originates from ϵ_z.

The theorem in Eq. (4) links the bunch lengths (or the radiation power) with the modulation strength (or the power of the laser modulator). Meanwhile, it can be alternatively presented as $|h| \geq \frac{\epsilon_y}{\sigma_{z\_y}(\mathrm{Mod})\sigma_z(\mathrm{Rad})}$. For a given radiation power or bunching factor, the product of $\sigma_{z\_y}(\mathrm{Mod})$ and $\sigma_z(\mathrm{Rad})$ is roughly decided. The demand for laser power or

ISBN: 978-3-95450-231-8 ISSN: 2673-5490 doi: 10.18429/JACoW-IPAC2023-MOPM065

modulation strength can then be mitigated by taking advantage of the ultra-small ϵ_y in a planar uncoupled storage ring. This is the exact gist of the GLSF scheme.

AN ILLUSTRATIVE INSTANCE

For illustration, a lattice-layout instance of a GLSF unit has been generated with practical magnet parameters. It is then tested for 'tracking', in which the particle coordinates of a launched Gaussian-distributed beam have been iterated turn-by-turn. Lattice components (parts 1-4) of the unit, together with the two halves of the ring outside, are represented by their linear transfer matrices. The modulation of M0 is assumed to be sinusoidal ($\Delta\delta = V_0 \sin(k_m z)$), while that of M1 and M2 is either linear ($\Delta\delta = hz$) or sinusoidal ($\lambda_m = 1\mu$m).

The test bunch is launched at the M0 center with a vertical emittance of 1 pm·rad. The initial RMS bunch length and natural energy spread are 50 nm and 2.5×10^{-4}. The bunch is then observed at the radiator center after 10^4 turns. When a linear modulation is applied at M1 and M2, a steady-state bunch length of 3 nm is attained, and the bunching factor at 13.5 nm is 0.372. The modulation strength is $|h| = 4000\,\mathrm{m}^{-1}$ and the power of the modulation laser is 1 MW. When the modulation waveform of M1 and M2 is sinusoidal, the beam distribution is distorted. The bunching factor at 13.5 nm, however, is still as large as 0.153. The produced radiation power can be calculated given the particle coordinates [8]. Assuming beam energy to be $E_s = 400$ MeV, average beam current $I = 1$ A, period number N_u and period length λ_u of the radiator undulator 160 and 1.25 cm, at 13.5 nm and within a ±2% bandwidth, the average EUV radiation power P_{rad} is 1.2 kW. Here, the power of the modulation laser is still 1 MW, which is what state-of-the-art optical cavities could bear in continuous-wave mode.

CONCLUSION

In this paper, we propose a generalized longitudinal strong focusing storage ring with steady-state nanometer-long electron bunches produced turn by turn, opening up possibilities for a variety of EUV-related applications. A practical instance implies that 1.2 kW quasi-continuous-wave 13.5-nm coherent EUV radiation can be obtained with a modulation laser power of 1 MW. Theories and methods to manage nonlinear dynamics issues based on the linear lattice concept presented here are still anticipated.

ACKNOWLEDGEMENTS

The authors thank Bocheng Jiang, Zhenghe Bai, Chao Feng, Yao Zhang, Xing Liu, Lixin Yan, Renkai Li, and Wenhui Huang for helpful discussions. This work is supported by the National Key R&D Program of China (Grant No. 2022YFA1603400) and the National Natural Science Foundation of China (NSFC Grant No. 12035010).

REFERENCES

[1] A. Damascelli, Z. Hussain, and Z. Shen, "Angle-resolved photoemission studies of the cuprate superconductors", *Rev. Mod. Phys.*, vol. 75, no. 2, pp. 473-541, 2003. doi:10.1103/RevModPhys.75.473

[2] V. Bakshi, *EUV lithography*, 2nd ed. Bellingham, USA: SPIE press, 2018.

[3] D. Ratner and A. Chao, "Steady-state microbunching in a storage ring for generating coherent radiation", *Phys. Rev. Lett.*, vol. 105, no. 15, p. 154801, 2010. doi:10.1103/PhysRevLett.105.154801

[4] A. Chao, E. Granados, X. Huang, H. Luo, and D. Ratner, "High Power Radiation Sources using the Steady-state Microbunching Mechanism", in *Proc. IPAC'16*, Busan, Korea, June 2016, pp. 1048-1053. doi:10.18429/JACoW-IPAC2016-TUXB01

[5] C. Tang *et al.*, "An Overview of the Progress on SSMB", in *Proc. FLS'18*, Shanghai, China, June 2018, pp. 166-170. doi:10.18429/JACoW-FLS2018-THP2WB02

[6] X. Deng *et al.*, "Experimental demonstration of the mechanism of steady-state microbunching", *Nature*, vol. 590, no. 7847, pp. 576–579, 2021. doi:10.1038/s41586-021-03203-0

[7] X. Deng, W. Huang, Z. Li, and C. Tang, "Harmonic generation and bunch compression based on transverse-longitudinal coupling", *Nucl. Instrum. Methods. Phys. Res., Sect. A*, vol. 1019, p. 165859, 2021. doi:10.1016/j.nima.2021.165859

[8] X. Deng *et al.*, "Average and statistical properties of coherent radiation from steady-state microbunching", *J. Synchrotron Rad.*, vol. 30, no. 1, pp. 35-50, 2023. doi:10.1107/S1600577522009973